

# ECG Denoising and Compression Using a Modified Extended Kalman Filter Structure

Omid Sayadi\*, *Student Member, IEEE*, and Mohammad Bagher Shamsollahi, *Member, IEEE*

**Abstract**—This paper presents efficient denoising and lossy compression schemes for electrocardiogram (ECG) signals based on a modified extended Kalman filter (EKF) structure. We have used a previously introduced two-dimensional EKF structure and modified its governing equations to be extended to a 17-dimensional case. The new EKF structure is used not only for denoising, but also for compression, since it provides estimation for each of the new 15 model parameters. Using these specific parameters, the signal is reconstructed with regard to the dynamical equations of the model. The performances of the proposed method are evaluated using standard denoising and compression efficiency measures. For denoising, the SNR improvement criterion is used, while for compression, we have considered the compression ratio (CR), the percentage area difference (PAD), and the weighted diagnostic distortion (WDD) measure. Several Massachusetts Institute of Technology–Beth Israel Deaconess Medical Center (MIT–BIH) ECG databases are used for performance evaluation. Simulation results illustrate that both applications can contribute to and enhance the clinical ECG data denoising and compression performance. For denoising, an average SNR improvement of 10.16 dB was achieved, which is 1.8 dB more than the next benchmark methods such as MABWT or EKF2. For compression, the algorithm was extended to include more than five Gaussian kernels. Results show a typical average CR of 11.37:1 with WDD < 1.73%. Consequently, the proposed framework is suitable for a hybrid system that integrates these algorithmic approaches for clean ECG data storage or transmission scenarios with high output SNRs, high CRs, and low distortions.

**Index Terms**—Denoising, ECG dynamical model (EDM), extended Kalman filter (EKF), hidden state variables, lossy compression.

## I. INTRODUCTION

ELECTROCARDIOGRAM (ECG) recordings obtained by a noninvasive technique is a harmless, safe, and quick method of cardiovascular diagnosis. The accuracy and content of information extracted from a recording require proper characterization of waveform morphologies, which, in turn, require the preservation of the phase and amplitude important clinical features and high attenuation of noise. ECG signals are usually corrupted with unwanted interference such as muscle noise, electrode artifacts, line noise, and respiration. On the other hand, efficient ECG compression techniques are desirable due to the huge amounts of digital data generated by ECG monitoring de-

VICES, and because the data need to be stored or transmitted over a communication channel [1]. In addition, certain transmission and storage methods can lead to segment corruption or packet loss, and therefore, dropouts missing data.

Several techniques have been proposed to extract the ECG components contaminated with the background noise and allow the measurement of subtle features in the ECG signal. One of the common approaches is the adaptive filter architecture, which has been used for the noise cancellation of ECGs containing baseline wander, electromyogram (EMG) noise, and motion artifacts [2], [3]. Statistical techniques such as principal component analysis [4], independent component analysis [5], [6], and neural networks [7] have also been used to extract a noise-free signal from the noisy ECG. Over the past several years, methods based on the wavelet transform (WT) have also received a great deal of attention for the denoising of signals that possess multiresolution characteristics such as the ECG [8]–[13].

Several ECG compression techniques have been developed within the last 30 years, most of which are based on lossy schemes for their higher compression ratio (CR) [14]. The compression techniques devised for ECG signals are classified into three different groups: direct, transformational, and parametric extraction methods [14], [15]. Most of the proposed schemes are based on the first two approaches. Hence, a few researchers have investigated the parametric extraction techniques.

On the other hand, a synthetic model has been proposed for generating artificial ECGs, which has unified the morphology and pulse timing in a single nonlinear dynamic model [16]. Concerning the simplicity and flexibility of this model, it can be easily used as a base for ECG processing, as demonstrated by Clifford *et al.* [17], where the use of the model to filter, compress, and classify the ECG was first proposed. This approach was based on the least squares error (LSE) optimization. The model may be further used in dynamic adaptive filters, such as the *Kalman Filter (KF)*. Sameni *et al.* proposed the use of a KF framework to update the model on a beat-to-beat basis in order to filter noisy ECGs [18]–[21]. The polar form of the dynamical equations was also used for Kalman-based ECG denoising [20].

In this paper, the KF framework has been further modified by adding 15 more equations to present the governing equations of the model parameters. In fact, the new proposed structure is aimed at estimating these new parameters, as well as the ECG signal. The added parameters are further used for reconstructing the ECG. Similar to [17], our proposed algorithm puts into work both the denoising and compression approaches simultaneously, but based on a sequential representation on a beat-by-beat dynamical adaptive basis. Meanwhile, the model is nonlinear and requires the nonlinear counterparts of the conventional Kalman filter. Our proposed model-based framework is built upon an extended Kalman filter (EKF) structure. Although there are several

Manuscript received May 4, 2007; revised August 25, 2007, November 14, 2007, December 31, 2007, and January 4, 2008. Asterisk indicates corresponding author.

\*O. Sayadi is with the Biomedical Signal and Image Processing Laboratory (BiSIPL), School of Electrical Engineering, Sharif University of Technology, Tehran 11365-9363, Iran (e-mail: osayadi@ee.sharif.edu).

M. B. Shamsollahi is with the Biomedical Signal and Image Processing Laboratory (BiSIPL), School of Electrical Engineering, Sharif University of Technology, Tehran 11365-9363, Iran (e-mail: mbshams@sharif.edu).

Digital Object Identifier 10.1109/TBME.2008.921150

Bayesian filters such as the extended Kalman smoother (EKS) and unscented Kalman filter (UKF), in this research, we have chosen the EKF for its simplicity and more numerical stability. However, the overall filtering performance is expected to be better with EKS or UKF.

The paper is organized as follows. Section II provides backgrounds on the EKF theory. Section III summarizes the ECG artificial model. In Section IV, the new complete EKF structure is proposed to incorporate the ECG dynamical model (EDM) parameters. In Section V, our proposed algorithm for denoising and compression is explained in details. Simulation results are provided in Section VI. Finally, discussion and conclusions are provided in Section VII.

## II. EXTENDED KALMAN FILTER REVIEW

The EKF is a nonlinear extension of conventional Kalman filter that has been specifically developed for systems having nonlinear dynamic models [22]. For a discrete nonlinear system with the state vector  $x_k$  and observation vector  $y_k$ , the dynamic model and its linear approximation near a desired reference point may be formulated as follows:

$$\begin{cases} \underline{x}_{k+1} = f(\underline{x}_k, \underline{w}_k, k) \\ \quad \approx f(\hat{\underline{x}}_k, \hat{\underline{w}}_k, k) + A_k(\underline{x}_k - \hat{\underline{x}}_k) + F_k(\underline{w}_k - \hat{\underline{w}}_k) \\ \underline{y}_k = g(\underline{x}_k, \underline{v}_k, k) \\ \quad \approx g(\hat{\underline{x}}_k, \hat{\underline{v}}_k, k) + C_k(\underline{x}_k - \hat{\underline{x}}_k) + G_k(\underline{v}_k - \hat{\underline{v}}_k) \end{cases} \quad (1)$$

where

$$\begin{aligned} A_k &= \left. \frac{\partial f(\underline{x}, \underline{w}, k)}{\partial \underline{x}} \right|_{\underline{x}=\hat{\underline{x}}_k} & F_k &= \left. \frac{\partial f(\hat{\underline{x}}_k, \underline{w}, k)}{\partial \underline{w}} \right|_{\underline{w}=\hat{\underline{w}}_k} \\ C_k &= \left. \frac{\partial g(\underline{x}, \underline{v}, k)}{\partial \underline{x}} \right|_{\underline{x}=\hat{\underline{x}}_k} & G_k &= \left. \frac{\partial g(\hat{\underline{x}}_k, \underline{v}, k)}{\partial \underline{v}} \right|_{\underline{v}=\hat{\underline{v}}_k} \end{aligned} \quad (2)$$

Here,  $w_k$  and  $v_k$  are the process and measurement noises, respectively, with covariance matrices  $Q_k = E\{w_k w_k^T\}$  and  $R_k = E\{v_k v_k^T\}$ . In order to implement the EKF, the time propagation and the measurement propagation equations are summarized as follows:

$$\begin{cases} \hat{\underline{x}}_{k+1}^- = f(\hat{\underline{x}}_k^+, \underline{w}, k)|_{\underline{w}=\underline{0}} \\ P_{k+1}^- = A_k P_k^+ A_k^T + F_k Q_k F_k^T \\ \hat{\underline{x}}_k^+ = \hat{\underline{x}}_k^- + K_k [y_k - g(\hat{\underline{x}}_k^-, \underline{v}, k)]|_{\underline{v}=\underline{0}} \\ K_k = P_k^- C_k^T [C_k P_k^- C_k^T + G_k]^{-1} \\ P_k^+ = P_k^- - K_k C_k P_k^- \end{cases} \quad (3)$$

where  $\hat{\underline{x}}_k^- = E\{\underline{x}_k | y_{k-1}, y_{k-2}, \dots, y_1\}$  is the *a priori* estimate of the state vector,  $x_k$ , at the  $k$ th update, using the observations  $y_1$  to  $y_{k-1}$ , and  $\hat{\underline{x}}_k^+ = \hat{E}\{\underline{x}_k | y_k, y_{k-1}, \dots, y_1\}$  is the *a posteriori* estimate of the state vector after adding the  $k$ th observations  $y_k$ .  $P_k^-$  and  $P_k^+$  are defined in the same manner to be the estimations of the covariance matrices in the  $k$ th stage, before and after using the  $k$ th observation, respectively.

## III. ECG DYNAMICAL MODEL

McSharry *et al.* [16] proposed a realistic synthetic ECG generator using a set of 3-D state equations that generates

a trajectory in the Cartesian coordinates. Sameni *et al.* [20] transformed these dynamic equations into the polar form to obtain a simpler compact set, with the simplified discrete form shown as:

$$\begin{cases} \theta_{k+1} = (\theta_k + \omega\delta) \bmod(2\pi) \\ z_{k+1} = - \sum_{i \in \{P, Q, R, S, T\}} \delta \frac{\alpha_i \omega}{b_i^2} \Delta\theta_i \exp\left(-\frac{\Delta\theta_i^2}{2b_i^2}\right) + z_k + \eta \end{cases} \quad (4)$$

where  $\delta$  is the sampling time,  $\alpha_i$ ,  $b_i$ ,  $\theta_i$  are the amplitude, angular spread, and location of the Gaussian functions, and  $\Delta\theta_i = (\theta - \theta_i) \bmod(2\pi)$  represents the RR interval variability. The ECG is then described by the set of discrete samples formed by  $z$ .  $\eta$  is a random additive white noise, which represents the baseline wander effects and models other additive sources of process noise [20]. As it is seen in (4), the palliative/provoking, quality, radiation, severity, timing (PQRST) waves are modeled with a sum of five Gaussian functions, each of which is located at a specific angular position  $\theta_i$ . In fact, the 3-D trajectory consists of a circular limit cycle in the polar plane, which is pushed up and down as it approaches each of the  $\theta_i$ . The projection of the trajectory on the  $z$ -axis gives a synthetic ECG.

## IV. PROPOSED COMPLETE EKF STRUCTURE TO INCORPORATE THE ECG MODEL PARAMETERS

In [19]–[21], the authors studied the application of EDM to ECG denoising using an EKF structure with only two state variables (which we call EKF2). In their works, they chose  $\theta$  and  $z$  as the only state variables. Hence, the state vector and the process noise vector were:

$$\begin{aligned} \underline{x}_k &= [\theta_k z_k]^T \\ \underline{w}_k &= [\alpha_P, \dots, \alpha_T, b_P, \dots, b_T, \theta_P, \dots, \theta_T, \omega, N]^T. \end{aligned} \quad (5)$$

Using the previous state variables, it is only possible to have estimations of the ECG (for example, in denoising applications) and the phase. Since these parameters are those that make the artificial ECG adaptable to different ECG signals, we have added the  $\alpha_i$ ,  $b_i$ , and  $\theta_i$  ( $i = P, Q, R, S$ , and  $T$ ) to the state variables and have proposed new dynamical equations for each. Long-term ECGs can be described by a series of states described by a given power-spectral density with similar parameters over the short term [23]. This idea motivated us to propose autoregressive (AR) dynamics as follows:

$$y_i[k+1] = \gamma y_i[k] + u_i[k] \quad (6)$$

where  $y_i$  denotes any of the 15 Gaussians' parameters  $\alpha_i$ ,  $b_i$ , and  $\theta_i$ , with  $u_i$  indicating its corresponding white noise. Regarding the small changes of the PQRST morphology during several cycles, we have adopted this AR model. In order to ensure a valid set of equations, we have set  $\gamma = 1$  (or  $\gamma \approx 1$ ), since the Gaussians' parameters are expected to have little variations from one beat to another beat in normal ECG signals. We expect that the recent sample of any of the newly introduced parameters can be regressed on the past value of itself to produce a useful estimate for the new sample. However, the AR (1) model also provides a noise term that accounts for the perturbations in morphology from beat to beat (such as those caused by respiration,

or changes in heart rate). For constructing the EKF structure, we have the new state vector and process noise vector as follows:

$$\begin{aligned} \underline{x}_k &= [\theta_k, z_k, \alpha_P, \dots, b_P, \dots, \theta_P, \dots, \theta_T]^T \\ \underline{w}_k &= [\omega, \eta, u_1, \dots, u_{15}]^T. \end{aligned} \quad (7)$$

With the 17 state variables in (7), the new modified EKF model is formulated as:

$$\begin{cases} \theta[k+1] = \theta[k] + \omega\delta = F_1(\theta_k, \omega, k) \\ z[k+1] = - \sum_{i \in \{P, Q, R, S, T\}} \delta \frac{\alpha_i[k]\omega}{b_i[k]^2} \Delta\theta_i[k] \exp\left(-\frac{\Delta\theta_i[k]^2}{2b_i[k]^2}\right) \\ \quad + z[k] + \eta = F_2(\theta_k, z_k, \alpha_{i_k}, b_{i_k}, \theta_{i_k}, N, k) \\ \alpha_P[k+1] = \alpha_P[k] + u_1[k] = F_3(\alpha_{P_k}, u_1, k) \\ \vdots \\ b_P[k+1] = b_P[k] + u_6[k] = F_8(b_{P_k}, u_6, k) \\ \vdots \\ \theta_P[k+1] = \theta_P[k] + u_{11}[k] = F_{13}(\theta_{P_k}, u_{11}, k) \\ \vdots \\ \theta_T[k+1] = \theta_T[k] + u_{15}[k] = F_{17}(\alpha_{T_k}, u_{15}, k). \end{cases} \quad (8)$$

The basic idea of the EKF is to linearize the state-space model (4) at each time instant around the most recent state estimation. Equation (9) represents the linearized version. Note that the terms which are equal to zero are not cited in this equation.

$$\begin{aligned} \frac{\partial F_1}{\partial \theta_k} &= 1, & \frac{\partial F_2}{\partial z_k} &= 1 \\ \frac{\partial F_2}{\partial \theta_k} &= - \sum_{i \in \{P, Q, R, S, T\}} \delta \frac{\alpha_i \omega}{b_i^2} \left[ 1 - \frac{\Delta\theta_i^2}{b_i^2} \right] \exp\left(-\frac{\Delta\theta_i^2}{2b_i^2}\right) \\ \frac{\partial F_2}{\partial \alpha_{i_k}} &= -\delta \frac{\omega}{b_i^2} \Delta\theta_i \exp\left(-\frac{\Delta\theta_i^2}{2b_i^2}\right) \\ \frac{\partial F_2}{\partial b_{i_k}} &= -2\delta \frac{\alpha_i \omega}{b_i^3} \Delta\theta_i \left[ 1 - \frac{\Delta\theta_i^2}{2b_i^2} \right] \exp\left(-\frac{\Delta\theta_i^2}{2b_i^2}\right) \\ \frac{\partial F_2}{\partial \theta_{i_k}} &= \delta \frac{\alpha_i \omega}{b_i^2} \left[ 1 - \frac{\Delta\theta_i^2}{2b_i^2} \right] \exp\left(-\frac{\Delta\theta_i^2}{2b_i^2}\right) \\ \frac{\partial F_3}{\partial \alpha_{P_k}} &= \frac{\partial F_4}{\partial \alpha_{Q_k}} = \frac{\partial F_5}{\partial \alpha_{R_k}} = \frac{\partial F_6}{\partial \alpha_{S_k}} = \frac{\partial F_7}{\partial \alpha_{T_k}} = 1 \\ \frac{\partial F_8}{\partial b_{P_k}} &= \frac{\partial F_9}{\partial b_{Q_k}} = \frac{\partial F_{10}}{\partial b_{R_k}} = \frac{\partial F_{11}}{\partial b_{S_k}} = \frac{\partial F_{12}}{\partial b_{T_k}} = 1 \\ \frac{\partial F_{13}}{\partial \theta_{P_k}} &= \frac{\partial F_{14}}{\partial \theta_{Q_k}} = \frac{\partial F_{15}}{\partial \theta_{R_k}} = \frac{\partial F_{16}}{\partial \theta_{S_k}} = \frac{\partial F_{17}}{\partial \theta_{T_k}} = 1. \end{aligned} \quad (9)$$

Having linearized the new modified EDM, an EKF may be developed. Note that in order to model the effects of the mismatch of the EDM with a true ECG signal, it is necessary to introduce a process noise in the dynamic model. For this, an additive random Gaussian white noise has been assumed in (8). This small portion of noise,  $\eta$ , gives more flexibility to the KF, and prevents it from converging to undesired limit cycles [4]. In the proposed EKF structure, we have only two noisy observations corresponding to the state variables  $\theta$  and  $z$  [21], which

are related to the state vector as follows:

$$\begin{bmatrix} \varphi_k \\ s_k \end{bmatrix} = \begin{bmatrix} 1 & 0 & 0 & \dots & 0 \\ 0 & 1 & 0 & \dots & 0 \end{bmatrix} \underline{x}_k + \begin{bmatrix} v_{1_k} \\ v_{2_k} \end{bmatrix} \quad (10)$$

where  $\varphi$  and  $s$  are the noisy observations corresponding to the phase and the ECG signal, respectively.  $v_1$  and  $v_2$  are the observation noises. Other state variables for which we have no observations are considered as the hidden states. In the EKF model, these variables would be estimated with respect to their dynamics given in (8). Also, we have  $R_k = E\{[v_{1_k}, v_{2_k}][v_{1_k}, v_{2_k}]^T\}$ . In the context of estimation theory, the variance of the observation noise in (10) somehow represents the degree of reliability of a single observation. In other words, when a rather precise measurement of the states of a system is valid, the value of  $R_k$  is low, and the Kalman filter gain is adapted such as to rely on that specific measurement. While for the epochs that the measurements are too noisy or there are no measurements available, the value of  $R_k$  is high and the Kalman filter tries to follow its underlying dynamics rather than relying on the observations.

## V. MODEL-BASED DENOSING AND COMPRESSION

Once the EKF structure is constructed, we can perform selected processing applications on ECG signals. The proposed framework can estimate any of its states according to the dynamical equations and the observations. In fact, they enable us to build up denoising and compression blocks, a concept that is addressed next.

### A. Denoising

The proposed nonlinear Bayesian framework estimates its variables using the state dynamical equations and its observations, noisy phase  $\varphi$  and noisy ECG  $s$ . Since the ECG signal,  $z$ , is a state variable in the EKF structure, the filtering procedure provides its estimation,  $\hat{x}_2$ , which is regarded as the denoised version of the input signal.

### B. Compression

A mathematical representation for the clean ECG signal can be obtained by integrating the last equation of the continuous form of EDM (1) with respect to  $t$  [16]. This way, the ECG signal is formulated as a sum of five Gaussians as:

$$z(a_i, b_i, \theta_i) = \sum_{i \in \{P, Q, R, S, T\}} \alpha_i \exp\left(-\frac{\Delta\theta_i^2}{2b_i^2}\right). \quad (11)$$

According to (11), if we have only an estimated value for the  $\alpha_i$ ,  $b_i$ , and  $\theta_i$ , we can reconstruct the original ECG. Since we have considered these variables as the states of EKF, we can easily estimate their values from  $\hat{\underline{x}}_{3:17}$ . But, the EKF updates its estimations when a new sample is observed. This means that the EKF estimates the  $\alpha_i$ ,  $b_i$ , and  $\theta_i$  parameters time series, in a similar manner to  $\theta$  and  $z$ . We expect a constant value for each of the 15 Gaussians' parameters during each heartbeat. This is especially true, because the amplitude, spread, and angular location of the PQRST do not vary within a single ECG beat. In practice, since the estimated series of  $\alpha_i$ ,  $b_i$ , and  $\theta_i$  are not a definitely constant function, we use its average value over each heartbeat

and use equation (12) to reconstruct the estimated ECG.

$$z_{\text{rec}} = \sum_{i=3:7} \hat{x}_i \exp\left(\frac{-[(\hat{x}_1 - \hat{x}_{i+10}) \bmod(2\pi)]^2}{2\hat{x}_{i+5}^2}\right). \quad (12)$$

This way, for every detected beat of an ECG, we must store/transmit 15 values. Also, as it can be seen from (12) that we need to store/transmit the estimated phase  $\hat{x}_1$  to be able to reconstruct the ECG. However, since the phase values are linearly distributed between  $-\pi$  and  $+\pi$ , we can only encode the zero locations (i.e., the R-peaks of  $\hat{x}_2$ ). In the decoder, we use these locations to assign the phase values between  $-\pi$  and  $+\pi$ .

A more accurate representation for reconstructing the compressed ECG through a sum of Gaussians is possible if we vary the number of Gaussian functions in (12). Clifford *et al.* proposed an extension of the EDM, which used an arbitrary number of Gaussians, with two Gaussians for each asymmetric turning point [17]. As was shown [24]–[26], using six–eight Gaussians is a more appropriate choice for the number of kernels used for reconstruction, but this would further affect the compression performance. We will discuss this point in the next section.

The proposal to use the EDM for compression was previously introduced an optimization scheme to find the LSE fit for the input ECG [17]. This fit was mathematically optimal in the LSE sense, but did not use any dynamical adaptable information about the input ECG. In the previous approach, the nonlinear optimization has to be performed within each cycle of the signal. Also, initial values of the parameters of the model are required. These initials together with the system dynamics (8) enable us to find an optimal fit for the proceeding cycles through the recursive solution (3). The current implementation is also based on the EDM. However, our method uses the dynamical set of equations in the construction of an adaptive filter, which not only uses the ECG as an observation but also depends on the state dynamics. Furthermore, the EKF-based algorithm does not need to have the initial parameters for every cycle of the input signal. Hence, the proposed EKF-based technique is an efficient idea for ECG compression.

## VI. RESULTS

The proposed algorithm implemented in Matlab on a Core Duo computer at 1.86 GHz with 1 Gb RAM. The same machine was used to measure processing time for the test signals. To study the performance of the proposed method several standard data sets from PhysioBank [27] were used, including the MIT-BIH normal sinus rhythm database (DB1) [28], the MIT-BIH noise stress test database (DB2) [29], the MIT-BIH arrhythmia database (DB3) [30], and the MIT-BIH compression test database (DB4) [31].

It is worth noting that the initial value for the state vector as well as the selection of the covariance matrices of the process and the measurement noise will highly influence the trajectory of the estimated vectors. Hence, prior to the implementation of the filter, it is necessary to select their values. In order to automate the parameter selection procedure for any given ECG, the parameters should be estimated from the signal itself. Similar to the approach discussed in [21], we have calculated the phase-

wrapped ECG for all phases between  $-\pi$  and  $\pi$ . Using the mean  $[\overline{\text{ECG}}(\theta)]$  and the standard deviation (SD)  $[\sigma_{\text{ECG}}(\theta)]$  of this new representation for the input signal, we are able to estimate the initial values for the dynamic model parameters using a typical nonlinear optimization scheme like *lsqnonlin.m* [32], [33], as proposed in [17]. It should be noted that the algorithm is highly affected by the choice of these initial values. Especially since the 15 Gaussians parameters need to be estimated only from two observations, errors in assigning their initial values cause the output of EKF not to follow the input ECG. Thus, the more precise the initial values are, the less the perturbation in the observations affects the filtering performance.

Similarly, the covariance values of  $Q_k$  are found by calculating the magnitude of the deviation of the parameters of the five Gaussian functions of EDM around the estimated mean, that best model the acceptable deviations of the ECG around  $\overline{\text{ECG}}(\theta)$ . This is again a nonlinear least-squares problem that is solved by finding the optimal parameters that generate the best fit of the mean ECG within the upper and lower ranges of  $\overline{\text{ECG}}(\theta) \pm \sigma_{\text{ECG}}(\theta)$ . We have used a global value for the angular frequency  $\omega$ , which is a simpler approximation for short signals with minor RR-interval deviations (between 10% to 20% [21]). This way, it may be set to  $\omega = 2\pi/\overline{T_{\text{RR}}}$ , where  $\overline{T_{\text{RR}}}$  is the average RR-interval of the whole signal. In a similar manner to [21], we set  $E\{v_{1k}^2\} = (\omega\delta)^2/12$ , and  $E\{v_{1k}^2\}$  is found from the deviations of the inactive segment of the ECG, between the end of the T-wave and the beginning of the next P-wave, which correspond to the ending segments of the phase-warped ECG.

Before presenting the experiments and results, the scope of the proposed filtering scheme needs to be further clarified. In the presented approach, due to the phase wrapping of the RR-interval to  $2\pi$ , normal interbeat variations of the RR-interval (between 10% to 20%), or consistent RR-interval abnormalities such as *Bradycardia* or *Tachycardia* do not considerably affect the filter performance. However, for morphological abnormalities that only appear in some of the ECG cycles, such as the *Premature Ventricular Contraction* (PVC), the phase error of the model can lead to large errors in the Gaussians function locations. Especially for low input SNRs, where neither the model nor the measurements are reliable for the filter, the filtering performance is not expected to be satisfactory. However, the benefit of the Gaussian mixture representation is that the effect of each Gaussian term vanishes very quickly (in less than the ECG period), meaning that the errors are not propagated to the following ECG cycles. Moreover, by monitoring the state estimates' covariance matrices and the variations of the innovation signals, it is possible to detect such unexpected abnormalities. Of course, it should be considered that the accurate filtering of abnormal ECGs with high morphologic changes, such as QT hysteresis and premature contraction beats, remains an open problem [21]. However, we are now studying EDM-based segmentation methods to extract the abnormal cycles of ECG signals. This way, it is possible to filter any ECG, if we can split the input signal into two or more signals with little morphological beat variation. The method proposed in [25] is another possibility. All these show the necessity of extensive and more accurate studies to develop a reliable technique to overcome mentioned problems.

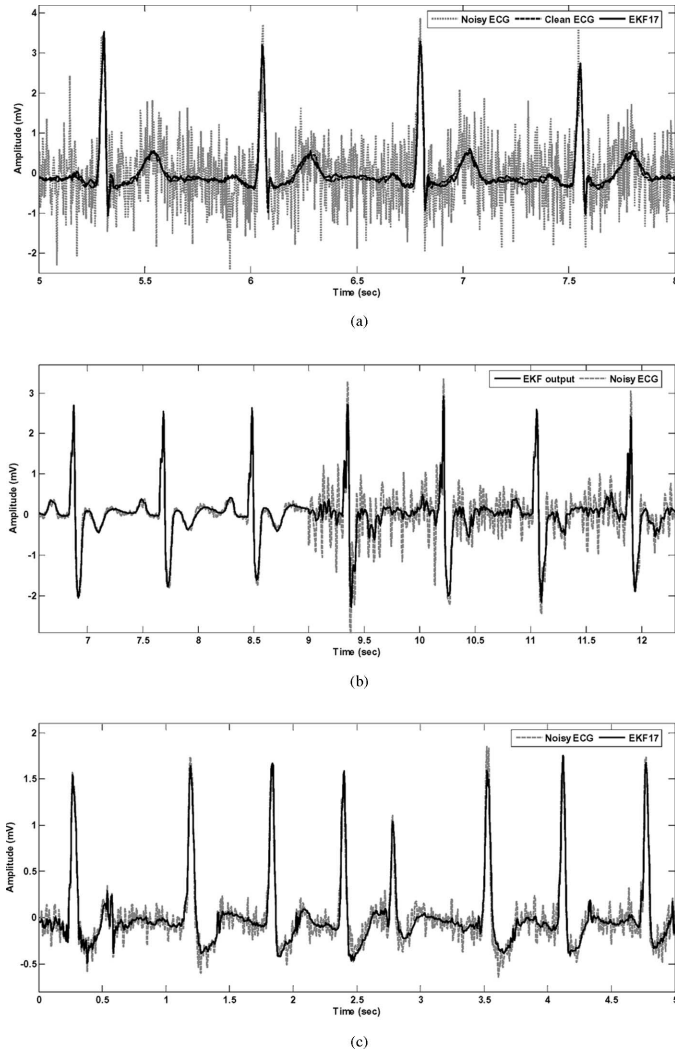


Fig. 1. Typical filtering results of EKF17 for different input ECGs. (a) Record 116 from DB3, with an additive white Gaussian noise of  $-2$  dB. (b) Record 118e24 from DB2, with calibrated amount of real EMG noise (corresponding to an input SNR of 2 dB for the noisy portion). (c) Record 203 from DB3, with real motion artifacts (corresponding to an input SNR of 5 dB).

### A. Denoising

The second estimation from the estimated states vectors obtained by the proposed EKF model with 17 state variables (EKF17) was chosen as the denoised signal. Three databases DB1, DB2, and DB3 were used to study the performance of the proposed method. Fig. 1 shows denoising results for different types of noises including white and real noises. As it can be seen, the denoised signal follows the clean ECG morphology when artificial white noise is added [see Fig. 1(a)]. Also, for the real EMG noises, the denoised signal is free from any EMG artifacts [see Fig. 1(b)]. Motion artifact is generally considered the most troublesome, since it can mimic the appearance of ectopic beats, it causes undesired notches on the ST segment and cannot be removed easily by simple bandpass filters, unlike other types.

Fig. 1(c) indicates that EKF17 is also able to remove motion artifact, while preserving diagnostic morphological information of the signal. Note that because there are underlying dynamics for the ECG signal, which constrain the filtering, motion artifact

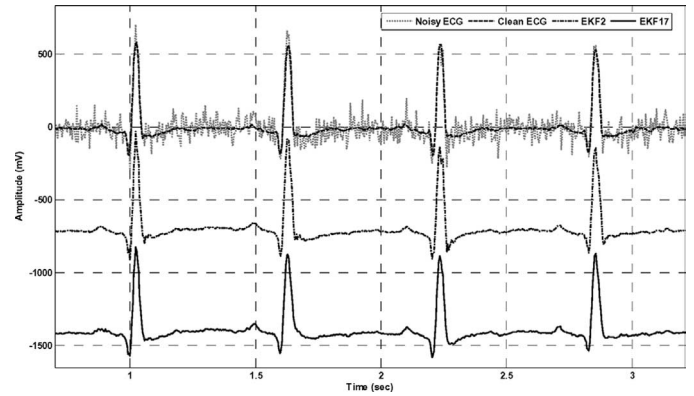


Fig. 2. Typical filtering results of EKF2 and EKF17 for an input signal of 5 dB using an additive white Gaussian noise (Record 16265 from DB1). The peaks distortions for EKF2 are clearly seen, especially in the ST segments and the R-peaks.

cannot force the denoised signal follow distorted waveforms. To clarify this, see Fig. 1(c), where the denoised signal shows a different pattern to that of the noisy signal. Specifically, the T-wave end points in the denoised signal do not follow the distorted T-wave end points of the noisy signal.

To appreciate the merits of EKF17 over the previously EKF model with two state variables (EKF2), we have illustrated the results of both methods in Fig. 2. One can easily find the peak distortions of EKF2, especially for the QRS complex, and the distortions in the ST segment.

For evaluating the performance of the proposed method, we have used the SNR improvement measure given by:

$$\text{imp[dB]} = \text{SNR}_{\text{output}} - \text{SNR}_{\text{input}} = 10 \log \left( \frac{\sum_i |x_n(i) - x(i)|^2}{\sum_i |x_d(i) - x(i)|^2} \right) \quad (13)$$

where  $x$  denotes the clean ECG,  $x_d$  is the denoised signal, and  $x_n$  represents the noisy ECG.

In order to investigate the performance of our algorithm and to compare it to different benchmark methods, we have implemented the EKF2 algorithm [21]. Also, a recently proposed algorithm based on the multiadaptive bionic WT (MABWT) [13], which has shown the best results among wavelet-based filtering techniques, has been implemented. Typical values for the SNR improvements of the ECG records of DB3 are provided in Table I. The analyzed portions of the records (in seconds) are also detailed in Table I. To ensure the consistency of the results, the whole procedure was repeated 100 times over the selected portions of the records of DB3 and the first 60 min of all 18 records of DB1; each time using a different set of random white Gaussian noise at the input. The SNRs were generally calculated over the second half of the filtered segments, to ensure that the transient effects of the filters would not influence the SNR calculations. For a quantitative comparison, the mean and SD of the SNR improvements versus different input SNRs is plotted in Fig. 3. Note the superiority of EKF17, especially in lower input SNRs, where the clean ECG is lost in noise.

### B. Compression

Having the estimations of the EKF state variables (7), the reconstructed ECG is obtained using (12). Fig. 4 shows an ECG

TABLE I  
PERFORMANCE EVALUATION OF THE BENCHMARK DENOISING ALGORITHMS ON DB3. THE VALUES SHOW SNR IMPROVEMENT IN DECIBELS

Input SNR	Algorithm	5 dB			0 dB			-5 dB		
		MABWT	EKF2	EKF17	MABWT	EKF2	EKF17	MABWT	EKF2	EKF17
111	0-55	6.28	5.88	8.91	6.76	6.40	8.65	6.92	8.70	9.48
113	0-60	7.52	7.46	8.59	7.63	8.08	9.15	8.00	8.98	10.00
115	0-60	7.75	7.44	8.04	8.20	8.39	9.51	8.33	8.95	10.11
116	0-60	7.14	6.97	8.61	7.37	7.09	9.13	7.76	7.12	9.63
117	0-60	7.42	7.29	8.85	7.69	7.73	9.71	8.08	7.82	10.21
121	20-80	8.75	8.58	9.72	8.98	9.09	10.61	9.27	9.23	11.14
122	0-60	7.64	7.47	8.74	7.87	7.71	9.64	8.26	7.79	10.15
123	0-60	8.27	8.10	9.14	8.50	8.66	9.93	8.89	8.87	10.52
124	10-70	7.10	6.93	8.61	7.33	7.09	9.15	7.72	7.15	9.63
231	10-70	6.58	6.41	8.28	6.81	8.06	9.79	7.20	8.75	10.71
Average:		7.44	7.25	8.75	7.71	7.83	9.53	8.04	8.34	10.16
SD:		0.73	0.77	0.46	0.71	0.81	0.54	0.71	0.79	0.52
Max:		8.75	8.58	9.72	8.98	9.59	10.61	9.27	9.23	11.14
Min:		6.28	5.88	8.04	6.76	6.40	8.65	6.92	7.12	9.48

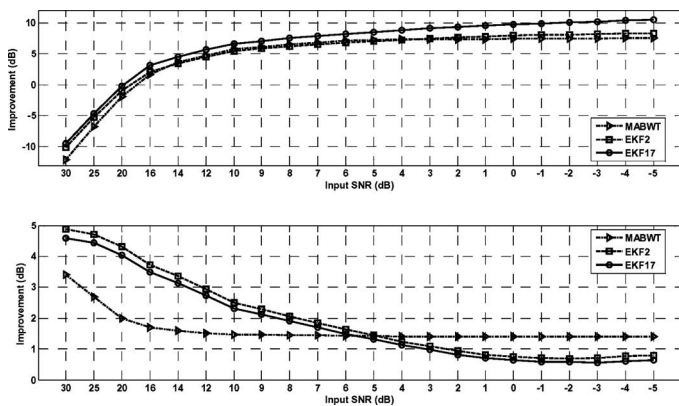


Fig. 3. The mean (top) and SD (bottom) of the filter output SNR improvements versus different input SNRs for the selected portions of the records of DB3 and the first 60 min of all 18 records of DB1, averaged over 100 repetitions for each of three methods; MABWT, EKF2, and EKF17.

signal, with 15 estimated Gaussians' parameters, i.e.,  $\hat{\alpha}_i$ ,  $\hat{b}_i$ ,  $\hat{\theta}_i$ , shown as time series. Note that they remain nearly constant valued during each normal beat. When the filter encounters a different rhythm, the Gaussian parameters change because the rhythm has been changed. This will cause their estimations not to remain constant anymore during that beat.

Using the parameters of the Gaussian functions of EDM, it is possible to reconstruct the input ECG. However, more accurate reconstruction is possible if we vary the number of Gaussian functions, as proposed by Clifford *et al.* [17], where asymmetries in waveforms, or extra waves (such as the U-wave) can be modeled by adding an extra Gaussian. Fig. 5 illustrates an ECG and the reconstructed signals using five and six Gaussians. As it can be seen, the signals are similar to the original ECG.

Particularly, when six Gaussians are used, the characteristic waveforms are reconstructed almost perfectly, with minimal distortion in the diagnostic information during compression. According to the asymmetric shape of the T-wave, for assigning the Gaussians to the PQRST waveforms, we used two Gaussians for the T-wave, called  $T^+$  and  $T^-$  [17]. This way, distortionless reconstruction of the T-wave and especially the ST segment is possible (see Fig. 5).

Database DB4 was used to evaluate the proposed compression algorithm and to compare it with other known compression methods. We have also implemented the embedded zero-trees of wavelet coefficients (EZW) method [34] based on the concept introduced in [35], and the set partitioning in hierarchical trees

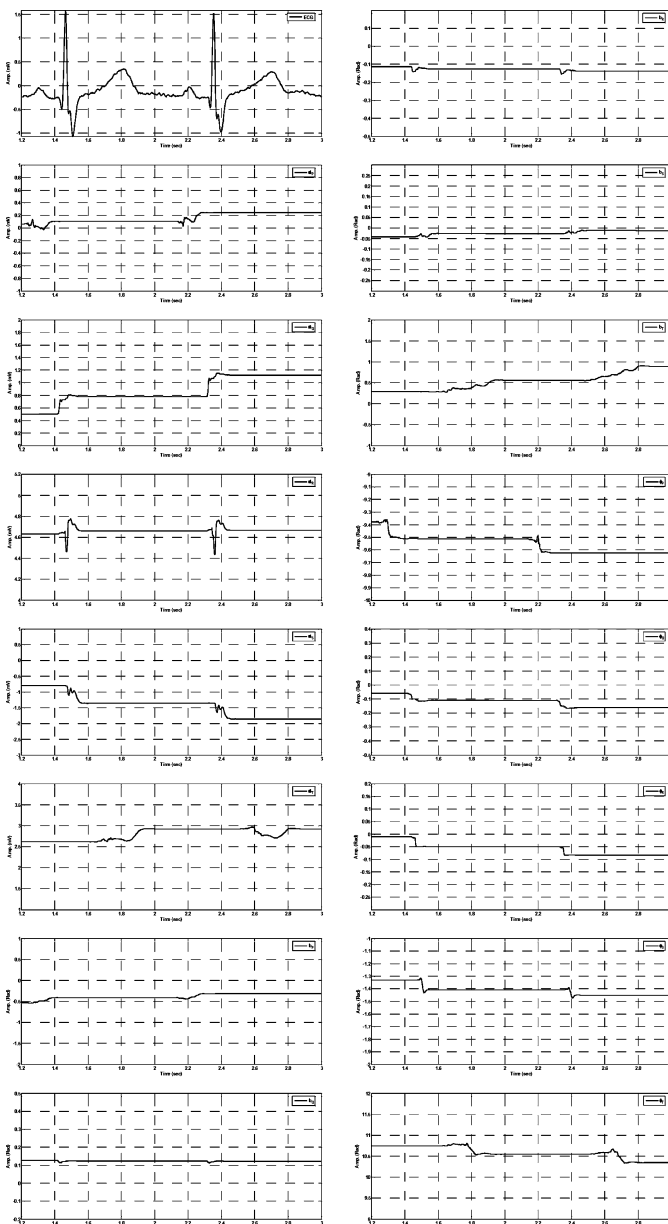


Fig. 4. Estimated Gaussians' parameters with EKF17 for record 231 from DB3 (analyzed portion 1.2 sec:3 sec).

(SPIHT) algorithm [36]. These compressors were chosen for comparison because they are often referred for comparison in the literature, and are known as the best transform-based ECG compressors. Generally speaking, most of the ECG compression algorithms use simple mathematical distortion measures such as the rms error, the percentage rms difference (PRD), the SNR, and a maximum amplitude error for evaluating the reconstructed signal [37]. Such performance indexes are irrelevant from the point of view of diagnosis [38]. In other words, all these error measures have disadvantages, which all result in poor diagnostic relevance. For example, if the signal has baseline fluctuations, the variance of the signal will be higher, the PRD will be artificially lower, and the SNR will be artificially higher. Furthermore, every segment in the PQRST complex has a different diagnostic meaning and significance. A given

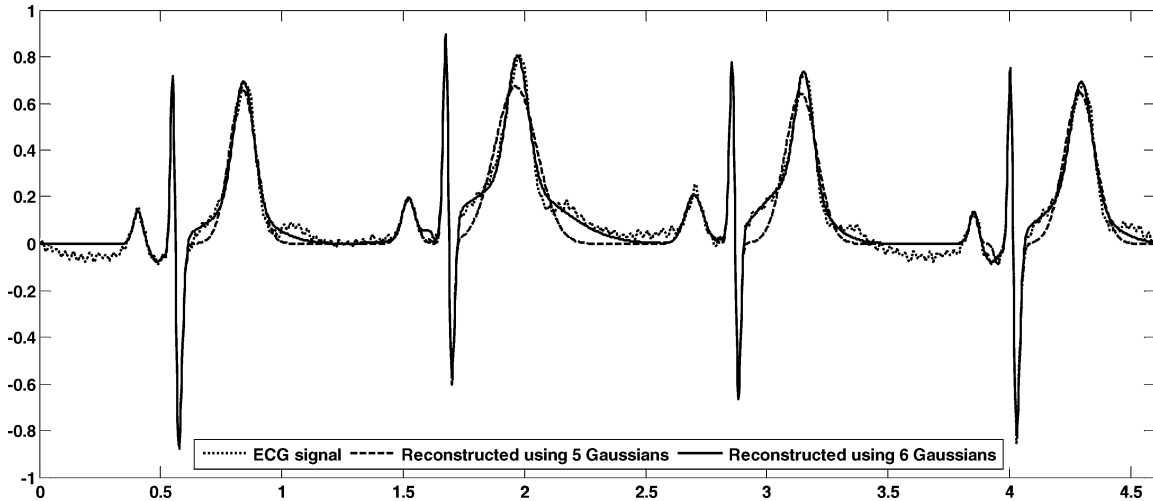


Fig. 5. Typical results of the EKF-based compression algorithms for Record 117 from DB3 (dotted line). The reconstructed signal using EKF17 (5 Gaussians) and EKF20 (6 Gaussians) are shown with dashed line and solid line, respectively.

distortion in one segment does not necessarily have the same relevance or importance as the same magnitude of distortion in another segment. For example, in many patients' ECGs, small changes (elevations or depressions) of the ST segment are much more diagnostically significant than the TP segment. In the proposed algorithm, we do not track the baseline since we are constructing the original ECG only through a sum of five or six Gaussians (12). Hence, the baseline of the reconstructed signal is expected to be flat. This can increase the error between the input ECG and the reconstructed one for nonflat portions and would increase the PRD value as well. To avoid such errors, baseline wanders have been eliminated using MABWT in the preprocessing stage.

The weighted diagnostic distortion (WDD) [38] is based on comparing the PQRST features of the original ECG and the reconstructed signal. The WDD measures the relative preservation of the diagnostic information in the reconstructed signal: the location, duration, amplitudes, and shapes of the waves and complexes that exist in every beat. It is defined as

$$\text{WDD}(\beta, \hat{\beta}) = \Delta\beta^T \frac{\Lambda}{\text{tr}(\Lambda)} \Delta\beta \times 100 \quad (14)$$

where  $\beta$  and  $\hat{\beta}$  represent two vectors of 18 diagnostic features of the original beat and reconstructed beat, respectively,  $\Delta\beta$  is the normalized difference vector, and  $\Lambda$  is a diagonal matrix of weights [38] which is set to

$$\Lambda = \text{diag}[2.5 \ 2.5 \ 1 \ 1 \ 2 \ 2 \ 1 \ 0.5 \ 0.1 \ \dots \ 1.5 \ 1 \ 3 \ 1.5 \ 1.5 \ 1 \ 1 \ 3 \ 3]. \quad (15)$$

In this research, we have used the same features and penalty matrices as [38]. We have also considered another error measure, called the percentage area difference (PAD) between the original and the reconstructed signal, which is defined for the time indexes between  $t_i$  and  $t_f$  as [39]:

$$\text{PAD} = \frac{\left| \int_{t_i}^{t_f} x(t) dt - \int_{t_i}^{t_f} x_r(t) dt \right|}{(t_f - t_i)(x_{\max} - x_{\min})} \times 100. \quad (16)$$

TABLE II  
PERFORMANCE EVALUATION OF BENCHMARK COMPRESSION ALGORITHMS ON DB4

Algorithm		Compression Performance Measures		
		CR:1	PAD (%)	WDD (%)
EZW		6.85±1.06	4.86±2.18	5.12±3.09
SPIHT		9.24±0.75	1.42±0.85	1.35±1.00
EKF	5 Gaussians (EKF17)	13.65±2.92	3.90±1.59	4.53±1.06
	6 Gaussians (EKF20)	11.37±2.48	1.07±0.74	1.73±0.71
	7 Gaussians (EKF23)	9.75±2.13	0.65±0.43	1.54±0.55
	8 Gaussians (EKF26)	8.53±1.87	0.42±0.24	0.96±0.33

Table II shows compression evaluation results for 50 selected records from DB4 with their complete durations. The results are compared to those of EZW and SPIHT. The CR for the model-based algorithm is formulated as:

$$\text{CR} = \frac{L}{n_{\text{param}}} = \frac{L}{(3n_{\text{Gauss}}n_{\text{beat}}) + n_R} \quad (17)$$

where  $L$  is the whole ECG length (in samples),  $n_{\text{param}}$  is the number of parameters required for reconstruction,  $n_{\text{beat}}$  is the total number of beats in the ECG sequence,  $n_{\text{Gauss}}$  is the number of Gaussian kernels used in the EDM, and  $n_R$  is the number of total R-peaks locations. Since  $n_R = n_{\text{beat}}$  the CR reduces to

$$\text{CR} = \frac{L}{n_{\text{beat}}(1 + 3n_{\text{Gauss}})}. \quad (18)$$

It can be seen from Table II that our proposed method provides a higher CR, while preserving the similarity between the original ECG and the reconstructed version most accurately. It is worth noting that in all cases, the WDD of EKF17 is comparable to and usually superior to the other methods being tested. Additionally, increasing the number of Gaussians results in lower CRs, as expected. Accordingly, EKF20 is chosen as the desired compression scheme because of its CR and low error measures.

Another interesting remark is that the CR of EKF-based algorithm depends upon the number of beats [refer to (18)]. This means that for ECG signals with lower average heart rates, the CR is much higher because the resulting ECG contains fewer

TABLE III  
HEART RATE AND SAMPLING FREQUENCY EFFECTS ON THE PERFORMANE  
OF EKF20 COMPRESSION ALGORITHM

Data-base	Record No.	$f_s$ (Hz)	Analyzed portion (sec)	Number of cycles	CR:1	WDD (%)
DB3	123	360	10-70	49	24.49	0.88
	231	360	10-70	64	18.75	3.19
	122	360	10-70	87	13.79	2.65
DB4	12621_01	213	0-24	23	12.37	2.02
	11442_01	213	0-24	30	9.48	1.23
	12247_01	213	0-24	46	6.18	1.50

beats. This is beneficial for compression of long-term ECGs, like Holter recordings. The CR is also a function of the sampling frequency  $f_s$ ; obviously, the CR for those signals with higher  $f_s$  would be higher. To simulate the heart rate and the sampling frequency effects on the CR, we have considered selected records from DB3 and DB4. The results for EKF20 are provided in Table III for EKF20. The results show the effect of heart rate on the CR. In fact, for a constant  $f_s$ , the more the number of beats are, the lower the CR is (see either second–fourth rows or fifth–seventh rows). Also, by comparing records that have approximately the same sampling frequency, we came to this conclusion that for a constant number of beats, the more the  $f_s$  is, the higher the CR is (compare the second row to the last row in which the number of beats are nearly equal).

The actual run time of the algorithms was used to evaluate the time complexity of the proposed method. Generally, by using  $m$  Gaussians kernels in (4), the state vector and the process noise vector in (7) have  $3m + 2$  entries, leading  $Q$ ,  $A$ , and  $F$  matrices to be  $(3m + 2) \times (3m + 2)$ .  $C$  is a  $(2) \times (3m + 2)$  matrix.

In addition,  $R$  and  $G$  matrices do not depend on the number of Gaussians. In other words, since we have two observations, these matrices are  $2 \times 2$ . Consequently, increasing  $m$  affects the dimensionality of the matrices and the run time. For a signal with approximately 20 000 samples (corresponding to almost 1 min at a sampling frequency of  $f_s = 360$  Hz), a run of EKF2, EKF17, EKF20, EKF23, and EKF26 takes about 12.2, 17.1, 21.7, 26.9, and 31.5 s, respectively.

## VII. DISCUSSION AND CONCLUSION

We have presented and validated a new EKF algorithm that incorporates the parameters of the EDM, and its applications to ECG denoising and compression. By introducing a simple AR model for each of the 15 dynamic parameters of the Gaussians, the new EKF structure was constructed. The proposed set of equations aims at integrating into the ECG model a mechanism that estimates the new hidden state variables without having any corresponding observations, which was later used for compression. The designed filter was applied to noisy ECG signals, and the results demonstrate the filter’s capability in tracking and filtering noisy ECG.

Compared to benchmark denoising schemes EKF2 and MABWT, EKF17 provides a larger SNR improvement, especially fewer input SNRs, where the original signal is lost in noise. Another point of interest is the low SD of SNR improvements for EKF17, which ensures the consistency of results as compared to other methods. Furthermore, the new modifications

in the EKF structure results in fewer peak distortions. Hence, the proposed method can serve as a base for the design of a robust ECG filter, with vast applications for low SNR ECGs.

The EKF structure not only estimates the clean ECG as a Kalman state variable, but also estimates the Gaussians parameters of the model. Therefore, a simple way to reconstruct the ECG is to store/transmit only these parameters, as well as the R-locations, for each beat. However, these estimations are not constant valued, and therefore, we have used their mean value over each beat (60 divided by the average heart rate). According to the described procedure, the ECGs were compressed and reconstructed using different number of Gaussian Kernels. It is worth noting that the results in this paper are for short ECGs. For longer ECGs, it is likely that the heart rate varies significantly, and therefore, the performance of the filter will vary. Long ECG sections will probably require an adaptive change of the parameters with the RR period.

For evaluating the performance of the proposed EKF-based algorithm for lossy compression and to give different weights to different diagnostic features, we used the WDD measure as the major distortion index. Its features depend on the PQRST waveforms, which qualify it to be the well-correlated measure with morphological characteristics of the ECG signal. Its only drawback is its expensive cost in term of time for calculation. Evaluation results showed that the proposed EKF-based algorithm has a high CR, while giving low WDD values (less than 5%). This means that the reconstructed signals can be guaranteed to be clinically useful provided that the initial values for the EKF structure are chosen appropriately. Another fact of the proposed EKF scheme is that the CR depends on the number of beats in the ECG signal. In other words, ECG signals with long RR-intervals result in a higher CR. This is more applicable to long-term ECG compression.

In addition, through simple modifications, the model would be robust to PQRST variations, which incorporates several pathological conditions such as small ST changes and QT prolongation. This gives the opportunity to study low amplitude complexes, even with interbeat changes. By modifying the simple model of (4) to incorporate more than five waves (P, Q, R, S, and T), except for the use of two Gaussians for the T-wave in EKF20, the error rate decreases (to less than 2%). But, the cost of using more Gaussian functions is a lowering of the CRs. The results showed that using six Gaussians (EKF20) can lead to an acceptable CR and WDD value.

Future works include incorporating baseline fluctuations in the EDM to reduce the distortions and cause the algorithm to be more reliable. In addition, different dynamical models may be proposed to represent the new state variables behavior. Also, it is possible not to use a constant value for the AR coefficient, but to find an adaptive value during different cycles. Moreover, lossless compression schemes may be proposed by combining EKF17 with a residual difference encoder [40].

## REFERENCES

- [1] G. M. Friesen, L. C. Jannett, M. A. Jadallah, S. L. Yates, S. R. Quint, and H. T. Nagle, “A comparison of the noise sensitivity of nine QRS detection algorithms,” *IEEE Trans. Biomed. Eng.*, vol. 37, no. 1, pp. 85–98, Jan. 1990.

- [2] N. V. Thakor and Y.-S. Zhu, "Applications of adaptive filtering to ECG analysis: Noise cancellation and arrhythmia detection," *IEEE Trans. Biomed. Eng.*, vol. 38, no. 8, pp. 785–794, Aug. 1991.
- [3] P. Laguna, R. Jane, O. Meste, P. W. Poon, P. Caminal, H. Rix, and N. V. Thakor, "Adaptive filter for event related bioelectric signals using an impulse correlated reference input: Comparison with signal averaging techniques," *IEEE Trans. Biomed. Eng.*, vol. 39, no. 10, pp. 1032–1044, Oct. 1992.
- [4] G. B. Moody and R. G. Mark, "QRS morphology representation and noise estimation using the Karhunen-Loève transform," in *Proc. Comput. Cardiology*, Jerusalem, Israel, Sep. 1989, pp. 269–272.
- [5] A. K. Barros, A. Mansour, and N. Ohnishi, "Removing artifacts from electrocardiographic signals using independent components analysis," *Neurocomputing*, vol. 22, no. 1–3, pp. 173–186, 1998.
- [6] T. He, G. D. Clifford, and L. Tarassenko, "Application of independent component analysis in removing artefacts from the electrocardiogram," *Neural Comput. Appl.*, vol. 15, pp. 105–116, 2006.
- [7] G. D. Clifford and L. Tarassenko, "One-pass training of optimal architecture auto-associative neural network for detecting ectopic beats," *Electron. Lett.*, vol. 37, no. 18, pp. 1126–1127, 2001.
- [8] K. Daqrouq, "ECG baseline wander reduction using discrete wavelet transform," *Asian J. Inf. Technol.*, vol. 4, no. 11, pp. 989–995, 2005.
- [9] H. A. Kestler, M. Haschka, W. Kratz *et al.*, "De-noising of high-resolution ECG signals by combining the discrete wavelet transform with the Wiener filter," in *Proc. Comput. Cardiology*, Cleveland, OH, Sep. 1998, pp. 233–236.
- [10] D. L. Donoho, "De-noising by soft-thresholding," *IEEE Trans. Inf. Theory*, vol. 41, no. 3, pp. 613–627, May 1995.
- [11] M. Popescu, P. Cristea, and A. Bezerianos, "High resolution ECG filtering using adaptive Bayesian wavelet shrinkage," in *Proc. Comput. Cardiology*, Cleveland, OH, Sep. 1998, pp. 401–404.
- [12] P. M. G. A. Da Silva and J. P. M. DeSa, "ECG noise filtering using wavelets with soft-thresholding methods," in *Proc. Comput. Cardiology*, Hannover, Germany, Sep. 1999, pp. 535–538.
- [13] O. Sayadi and M. B. Shamsollahi, "Multiadaptive bionic wavelet transform: Application to ECG denoising and baseline wandering reduction," *EURASIP J. Adv. Signal Process.*, vol. 2007, pp. 1–11, 2007.
- [14] S. M. S. Jaleddine, C. G. Hutgens, R. D. Strattan, and W. A. Coberly, "ECG data compression techniques—A unified approach," *IEEE Trans. Biomed. Eng.*, vol. 37, no. 4, pp. 329–343, Apr. 1990.
- [15] M. Blanco-Velasco, F. Cruz-Roldan, F. Lopez-Ferreras, A. Bravo-Santos, and D. Martinez-Munoz, "A low complexity algorithm for ECG signal compression," *Med. Eng. Phys.*, vol. 26, no. 7, pp. 553–568, Sep. 2004.
- [16] P. E. McSharry, G. D. Clifford, L. Tarassenko, and L. A. Smith, "A dynamic model for generating synthetic electrocardiogram signals," *IEEE Trans. Biomed. Eng.*, vol. 50, no. 3, pp. 289–294, Mar. 2003.
- [17] G. D. Clifford, A. Shoeb, P. E. McSharry, and B. A. Janz, "Model-based filtering, compression and classification of the ECG," *Int. J. Bioelectromagnetics*, vol. 7, no. 1, pp. 158–161, 2005.
- [18] M. Mneimneh, E. Yaz, M. Johnson, and R. Povinelli, "An adaptive kalman filter for removing baseline wandering in ECG signals," in *Proc. 33rd Annu. Int. Conf. Comput. Cardiol.*, 2006, pp. 253–256.
- [19] R. Sameni, M. B. Shamsollahi, and C. Jutten, "Filtering electrocardiogram signals using the extended Kalman filter," in *Proc. 27th Annu. Int. Conf. IEEE Eng. Med. Biol. Soc. (EMBS)*, Shanghai, China, Sep. 1–4, 2005, pp. 5639–5642.
- [20] R. Sameni, M. B. Shamsollahi, C. Jutten, and M. Babaie-Zadeh, "Filtering noisy ECG signals using the extended Kalman filter based on a modified dynamic ECG model," in *Proc. 32nd Annu. Int. Conf. Comput. Cardiol.*, Lyon, France, Sep. 25–28, 2005, pp. 1017–1020.
- [21] R. Sameni, M. B. Shamsollahi, C. Jutten, and G. D. Clifford, "A nonlinear bayesian filtering framework for ECG denoising," *IEEE Trans. Biomed. Eng.*, vol. 54, no. 12, pp. 2172–2185, Dec. 2007.
- [22] S. M. Kay, *Fundamentals of Statistical Signal Processing: Estimation Theory*. Englewood Cliffs, NJ: Prentice-Hall, 1993.
- [23] P. E. McSharry and G. D. Clifford, "A statistical model of the sleep-wake dynamics of the cardiac rhythm," *Comput. Cardiol.*, vol. 32, pp. 591–594, Sep. 2005.
- [24] G. D. Clifford and P. E. McSharry, "Method to filter ECGs and evaluate clinical parameter distortion using realistic ECG model parameter fitting," *Comput. Cardiol.*, vol. 32, pp. 735–738, Sep. 2005.
- [25] G. D. Clifford, "A novel framework for signal representation and source separation: Applications to filtering and segmentation of biosignals," *J. Biol. Syst.*, vol. 14, no. 2, pp. 169–183, Jun. 2006.
- [26] G. D. Clifford and M. Villarroel, "Model-based determination of QT intervals," *Comput. Cardiol.*, vol. 33, pp. 357–360, Sep. 2006.
- [27] PhysioBank, physiologic signal archives for biomedical research [Online]. Available: <http://www.physionet.org/physiobank/>
- [28] The MIT-BIH Normal Sinus Rhythm Database [Online]. Available: <http://www.physionet.org/physiobank/database/nsrdb/>
- [29] The MIT-BIH Noise Stress Test Database [Online]. Available: <http://www.physionet.org/physiobank/database/nstdb/>
- [30] The MIT-BIH Arrhythmia Database [Online]. Available: <http://www.physionet.org/physiobank/database/mitdb/>
- [31] The MIT-BIH Compression Test Database [Online]. Available: <http://www.physionet.org/physiobank/database/cdb/>
- [32] T. F. Coleman and Y. Li, "On the convergence of reflective Newton methods for large-scale nonlinear minimization subject to bounds," *Math. Program.*, vol. 67, no. 2, pp. 189–224, 1994.
- [33] T. F. Coleman and Y. Li, "An interior, trust region approach for nonlinear minimization subject to bounds," *SIAM J. Optim.*, vol. 6, pp. 418–445, 1996.
- [34] M. L. Hilton, "Wavelet and wavelet packets compression of electrocardiogram," *IEEE Trans. Biomed. Eng.*, vol. 44, no. 5, pp. 394–402, May 1997.
- [35] J. A. Norris, K. B. Englehart, and D. F. Lovely, "Myoelectric signal compression using zerotrees of wavelets coefficients," *Med. Eng. Phys.*, vol. 25, no. 9, pp. 739–746, Nov. 2003.
- [36] Z. Lu, D. Y. Kim, and W. A. Pearlman, "Wavelet compression of ECG signals by the set partitioning in hierarchical trees algorithm," *IEEE Trans. Biomed. Eng.*, vol. 47, no. 7, pp. 849–856, Jul. 2000.
- [37] M. Ishijima, "Fundamentals of the decision of optimum factors in the ECG data compression," *IEICE Trans. Inf. Sys.*, vol. E76-D, no. 12, Dec. 1993.
- [38] Y. Zigel, A. Cohen, and A. Katz, "The weighted diagnostic distortion measure for ECG signal compression," *IEEE Trans. Biomed. Eng.*, vol. 47, no. 11, pp. 1422–1430, Nov. 2000.
- [39] A. C. D'Ambrosio, A. Ortiz-Conde, and F. J. G. Sánchez, "Percentage area difference (PAD) as a measure of distortion and its use in maximum enclosed area (MEA), a new ECG signal compression algorithm," in *Proc. 4th IEEE Int. Caracas Conf. Devices, Circuits Syst.*, Aruba, Apr. 17–19, 2002, pp. 1035–1–1035-5.
- [40] R. Kannan and C. Eswaran, "Lossless compression schemes for ECG signals using neural network predictors," *EURASIP J. Adv. Signal Process.*, vol. 2007, Article ID 35641, pp. 102–122, 2007, doi:10.1155/2007/35641.



**Omid Sayadi** (S'06) was born in Shiraz, Iran, in 1983. He received the B.Sc. degree in biomedical engineering from Shahed University, Tehran, Iran, in 2005, and the M.Sc. degree in electrical engineering, biomedical engineering in 2007 from Sharif University of Technology, Tehran, where he is currently working toward the Ph.D. degree in biomedical engineering at the Electrical Engineering Department.

He is also a member of Biomedical Signal and Image Processing Laboratory (BiSIPL), Sharif University of Technology. His current research interests

include dynamical models for ECG generation, model-based ECG processing, the application of wavelet concepts, and especially multiadaptive bionic wavelet transform to biomedical signal processing solutions, signature verification, and efficient heart modeling.



**Mohammad Bagher Shamsollahi** (M'02) was born in Qom, Iran, in 1965. He received the B.Sc. degree in electrical engineering from Tehran University, Tehran, Iran, in 1988, the M.Sc. degree in electrical engineering, telecommunications from Sharif University of Technology, Tehran, in 1991, and the Ph.D. degree in electrical engineering, biomedical signal processing from the University of Rennes 1, Rennes, France, in 1997.

Currently, he is an Associate Professor in the Department of Electrical Engineering, Sharif University of Technology. His current research interests include biomedical signal processing, brain computer interface, and time-scale and time-frequency signal processing.